Stress Analysis and Fatigue of Weldments

A.B. Chattopadhyay[1], G. Glinka[1], S. Malik[1]
[1]University of Waterloo, Waterloo, Canada;

Introduction

Fatigue life estimation for welded structures requires knowledge of the stress field at the critical locations. The proposed method allows for the determination of the stress distribution in the weld toe region using a shell finite element model. The region of interst must be meshed such that the gradient of the through-thickness stress is captured. The stress data obtained via the shell finite element model is then modified via stress concentration factors to obtain peak stress values and estimate the fatigue life of a component. The stress distribution obtained using this method may also be used for fatigue crack growth analyses. One type of welded joint was used to validate the proposed method: a Desmoines T-joint welded connection. The reference stresses for these geometries were obtained using finely-meshed three-dimensional finite-element models. The shell finite element model was found to be in good agreement with the results from the three-dimensional finite-element models.

1 The hot spot stress and the stress concentration factor

The nominal stress, σ_n, in a plate without any attachments and notches would be equal to the stress found using a simple tension or bending stress formula. The existence of the attachment changes the stiffness in the weld toe region resulting in the stress concentration by creating a stress spike near the weld toe region. However, the nominal stress in both these cases would be the same. Determining a meaningful and unique nominal stress in complex welded structures is difficult, however, so the structural stress, σ_{hs}, also known as the 'hot spot stress' is often used. The hot spot stress has the advantage of accounting for the global geometry of the structure and the existence of the weld, but it does not account for the micro-geometrical effects such as the weld toe radius, r, and weld angle, Θ.

The same hot spot stresses ($\sigma_{hs}^{1,a} = \sigma_{hs}^{1,b}$) may result in different stress concentrations and different peak stresses, σ_{peak}. For this reason the hot spot stress alone is not good enough for the determination of the load independent stress concentration factors. In order to define a unique stress concentration factor dependent on the geometry only, both the magnitude and the gradient of the linearized (hot spot) stress must be accounted for. Niemi [3] proposed a method to decompose the linearized through-thickness stress field into a uniformly distributed membrane (axial) stress field, σ_{hs}^{m}, and an antisymmetric bending field, σ_{hs}^{b}. This concept is very useful because it captures the gradient ($\sigma_{hs}^{m}/\sigma_{hs}^{b}$) of the hot spot stress. However, in order to determine the magnitude of the peak stress, the stress concentration for pure axial load ($K_{t,hs}^{m}$) and pure bending load ($K_{t,hs}^{b}$) are necessary. The advantage of using the stress concentrations $K_{t,hs}^{m}$ and

$K^b_{t,hs}$ lies in the fact that they are independent of the load magnitude and are unique for a given geometry. In addition, the nominal stresses and the hot spot stresses for pure axial loading are equal to each other. This also holds true for the nominal and hot spot stresses generated in pure bending. As a result of this, the classical stress concentration factors based on the nominal stress can be used. The peak stress, σ_{peak}, can be expressed as the sum of the membrane and pure bending contributions.

$$\sigma_{peak} = \sigma^m_{hs} \cdot K^m_{t,hs} + \sigma^b_{hs} \cdot K^b_{t,hs} \qquad (1)$$

However, in order to determine the peak stress, σ_{peak}, the hot spot stresses σ^m_{hs} and σ^b_{hs}, as well as the appropriate stress concentration factors $K^m_{t,hs}$ and $K^b_{t,hs}$ must be known. It is appropriate at this moment to clarify the difference between the linearized stress field and the classical nominal stress and various stress concentration factors often used while analyzing notched mechanical and structural components.

2 Stress concentration factors for butt and fillet welds

Because under pure axial and pure bending load the nominal stress and the hot spot stress are the same ($\sigma^m_{hs} = \sigma^m_n$ and $\sigma^b_{hs} = \sigma^b_n$) the classical stress concentration factors can be used for the determination of the peak stress (eq. 1) at the weld toe. A literature search was carried out [4-7] and several stress concentration factors solutions were compared with each other and verified using in-house finite element data. The most universal were found to be stress concentration factors supplied by Japanese researchers [7] and they are discussed below. The quantities in the expressions are shown in Figure 1.

— Stress concentration factor near one-sided fillet weld under axial load.

$$K^m_{t,hs} = 1 + \frac{1 - \exp\left(-0.9\theta\sqrt{\frac{W}{2h}}\right)}{1 - \exp\left(-0.45\pi\sqrt{\frac{W}{2h}}\right)} \times \left[\frac{1}{2.8\left(\frac{W}{t}\right) - 2} \times \frac{h}{r}\right]^{0.65} \qquad \text{-tension} \qquad (2)$$

— Stress concentration factor near one-sided fillet weld under bending load.

$$K_{t,hs}^{b} = 1 + \frac{1-\exp\left(-0.9\theta\sqrt{\frac{W}{2h}}\right)}{1-\exp\left(-0.45\pi\sqrt{\frac{W}{2h}}\right)} \times 1.9\sqrt{\tanh\left(\frac{2t_p}{t+2h}+\frac{2r}{t}\right)} \times \tanh\left[\frac{\left(\frac{2h}{t}\right)^{0.25}}{1-\frac{r}{t}}\right] \times \left[\frac{0.13+0.65\left(\frac{r}{t}\right)^{4}}{\left(\frac{r}{t}\right)^{\frac{1}{3}}}\right] \quad \text{-bending} \qquad (3)$$

where: $W = (t+2h) + 0.3(t_p + 2h)$

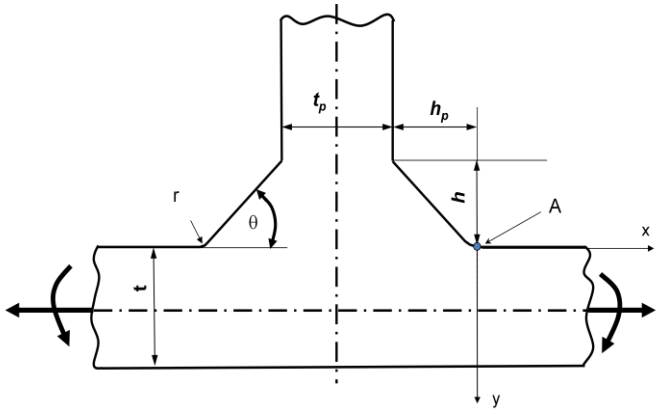

Fig.1 Example of dimensions for stress concentration factor equations

Expressions (2) and (3) are empirical in nature and have been derived using extensive finite element stress concentration database. Their application was verified for a range of geometrical configurations limited to $0.02 \le r/t \le 0.16$ and $30^o \le \theta \le 60^o$.

3 The through-thickness stress distribution

Detail knowledge of the through the thickness stress distribution, $\sigma(y)$, in the critical cross section is necessary for the analysis of fatigue crack growth emanating from the weld toe. The hot spot stresses, σ_{hs}^{m}, and, σ_{hs}^{b}, are sufficient for the determination of only the peak stress, σ_{peak}, at the weld toe. Useful generalized through-thickness stress distributions for T-butt welded joints were derived by Monahan [8]. Monahan's equation is expressed in (Eq.4)

$$\sigma(y) = \sigma(y)^m + \sigma(y)^b$$
$$= \left[\frac{K_{t,hs}^m \sigma_{hs}^m}{2\sqrt{2}} \cdot \frac{1}{G_m} + \frac{K_{t,hs}^b \sigma_{hs}^b}{2\sqrt{2}} \cdot \frac{1-2\left(\frac{y}{t}\right)}{G_b} \right] \left[\left(\frac{y}{\rho} + \frac{1}{2} \right)^{-\frac{1}{2}} + \frac{1}{2} \left(\frac{y}{\rho} + \frac{1}{2} \right)^{-\frac{3}{2}} \right] \quad (4)$$

where:

$$G_m = 1 \quad for \quad \frac{y}{r} \le 0.3$$

$$G_m = 0.06 + \frac{0.94 \times e^{-E_m T_m}}{1 + E_m^3 T_m^{0.8} \times e^{-E_m T_m^{1.1}}} \quad for \quad \frac{y}{r} > 0.3$$

$$E_m = 1.05 \times \theta^{0.18} \left(\frac{r}{t} \right)^q$$

$$q = -0.12\Theta^{-0.62}$$

$$T_m = \frac{y}{t} - 0.3\frac{y}{t}.$$

$$G_b = 1 \quad for \quad \frac{y}{r} \le 0.4$$

$$G_b = 0.07 + \frac{0.93 \times e^{-E_b T_b}}{1 + E_b^3 T_b^{0.6} \times e^{-E_b T_b^{1.2}}} \quad for \quad \frac{y}{r} > 0.4$$

$$E_b = 0.9 \left(\frac{r}{t} \right)^{-\left(0.0026 + \frac{0.0825}{\theta}\right)} \quad and \quad T_b = \frac{y}{t} - 0.4\frac{r}{t}.$$

The stress concentration factors $K_{t,hs}^m$ and $K_{t,hs}^b$ are available already in the form of expressions (2-3). Therefore a method is needed for obtaining the membrane and bending hot spot stresses σ_{hs}^m and σ_{hs}^b respectively.

4 The shell finite element model

The membrane and bending hot spot stresses are determined as follows:

$$\sigma_{hs}^{m} = \frac{\sigma_{hs}^{1} + \sigma_{hs}^{2}}{2} \tag{5}$$

$$\sigma_{hs}^{m} = \frac{\sigma_{hs}^{1} - \sigma_{hs}^{2}}{2} \tag{6}$$

A simple element model such as the one shown in Fig. 2b is not capable of supplying sufficiently accurate stresses in the weld toe region. This is because the critical cross section in the actual welded joint is located at the weld toe (section A and B, Fig. 2). The magnitude of stresses σ_{hs}^{1} and σ_{hs}^{2} and the resultant slope of the linear stress field depend on the distance from the point 'O' (Fig. 2b) and the size of the shell element.

The shell stresses in the weld toe region depend strongly on the local stiffness of the joint and therefore they are sensitive to how the weld stiffness is accounted for in the finite element shell model. It is important to model the weld and the structure in such a way that the hot spot shell membrane stress σ_{hs}^{m} and bending stress σ_{hs}^{b} in the critical cross sections (Fig. 2b) are the same as those which would be determined from the linearization of the actual 3D stress fields obtained analytically or from a finely mesh 3D finite element model of the joint. Fayard, Bignonnet, and Dang Van [9] proposed a shell finite element model with rigid bars simulating the weld. They also formulated a set of rules concerning the finite element meshing in order to correctly capture the properties of the linear stress field. However, using shell elements and rigid bars was found to be inconvenient in practice. A new model involving weld shell elements of the same type as the rest of the structure was therefore proposed.

The most important issues concerning the shell finite element modeling of welded joints is the location of the stress reference point, where the stress characterizing the linearized stress field in the weld toe cross section is to be determined. The shell finite element model has to be constructed in such a way that the location of the stress reference point coincides with the actual weld toe position (Fig. 2). In order to assure that the global effects of the joint geometry and the weld are adequately modeled, a set of rules have been formulated concerning the construction of an appropriate finite element shell model.

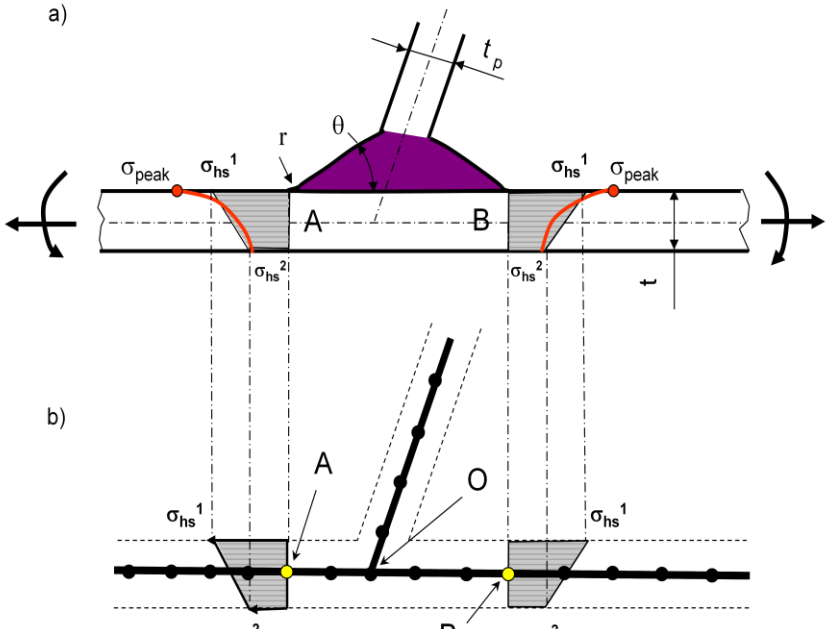

Fig.2 A welded joint and its simple shell finite element model: (a) Welded joint and stress distributions in critical cross sections; (b) shell finite element model and resultant stress distributions

a) Connect the mid-thickness planes shown in Figure 3a and Figure 3b (shown as solid thick lines) and add one layer of inclined elements representing the weld.

b) The first and the second row of elements in both plates adjacent to the theoretical intersection line (point 'O') of the mid-thickness planes must be of the size of $(t_p+h)/4$ in the 'x' direction for elements in the main plate and (t+h)/4 in the y direction for elements in the attachment. The shell elements simulating the weld are then attached to each plate in the middle of the weld leg length and they are spanning the first two rows of elements adjacent in each plate to the intersection point 'O'. The thickness of the shell elements simulating the weld is recommended to be equal to the thickness of the thinner plate being connected by the weld (i.e. either t or t_p whichever is less). The shell elements simulating the weld should have the same thickness. All shell elements in the weld region have the same dimension in the 'z' direction which is equal to the half of the weld leg length 'h/2' or less.

c) The elements in the third row from point 'O' should have the size equal to the half weld leg length 'h/2' in the 'x' and 'z' direction for elements simulating the main plate and the same 'h/2' dimension in the y and z direction for elements in the attachment plate. The choice of such dimensions enables to locate the stress reference point 'A' at nodal points of elements in the third row. The location of the stress reference point 'A' must and it does coincide in such a case with the physical location of the weld toe. Thus stresses at the reference point A are the same as the nodal stresses and they can be extracted without any interpolation or additional post-processing.

d) The size 'z' of the first two rows of elements adjacent to the intersection point 'O' is dictated by the size of the smallest element in the region, i.e. it should not be greater than half of the weld

leg length ‘h/2’. It means that the first and the second row of elements in the main plate have the dimension [(h/4+t_p/4)×h/2] and the first two rows of elements in the attachment should have the size of [(h/4+t/4)×h/2]. The elements in the third row are (h/2×h/2) in size. The spacing in the ‘z’ direction might need to be smaller than half of the weld leg length ‘h/2’ while modeling rounded corners of non-circular tubes and weld ends around gusset plates.

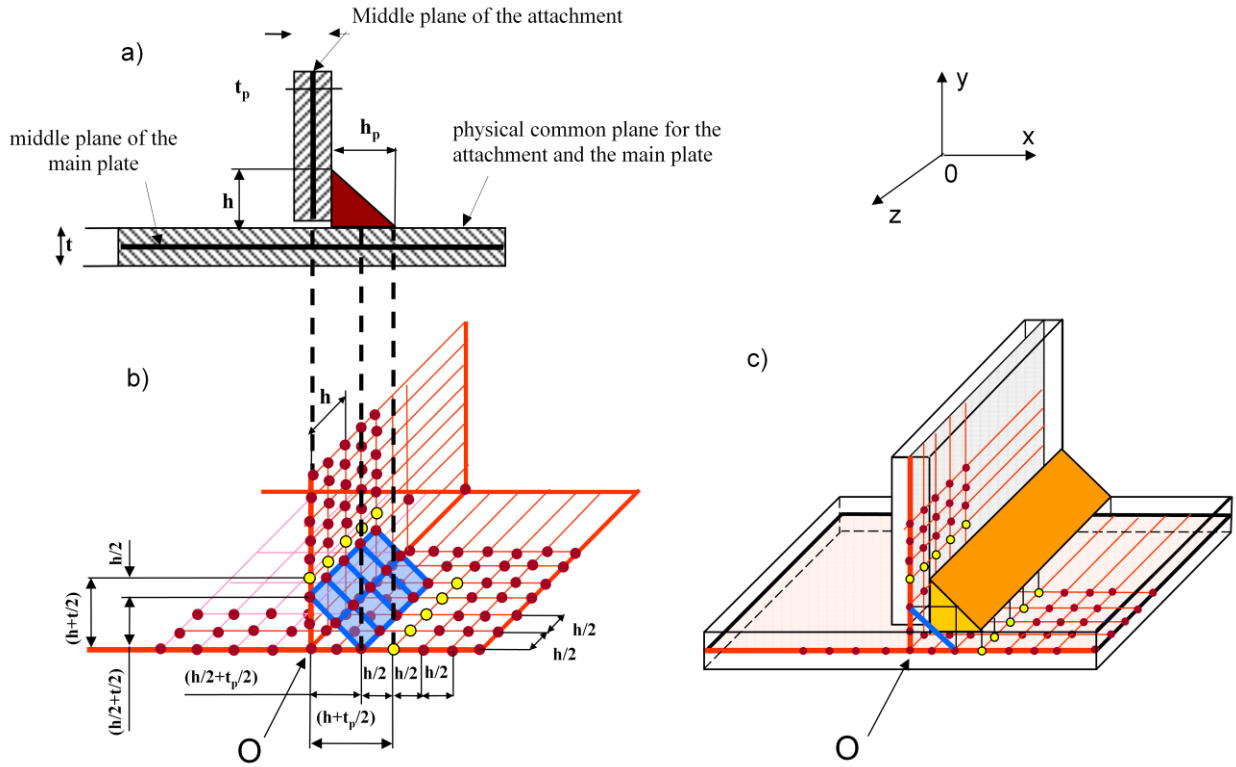

Fig.3 A welded joint and its simple shell finite element model: (a) welded joint and stress distribution in critical cross sections; (b) shell finite element model and resultant stress distribution; (c) superposition of the actual welded joint and its shell finite element model

5 Numerical Validation: Desmoines Welded T-Joint

A Desmoines welded T-joint subjected to a torque applied to the tube via a bolted plate subjected to a load (Fig. 4) was analyzed by using both a finely-meshed 3D finite element model and a shell finite element model. Apart from the four bolted connections where the torque was applied, the structure was bolted to the ground. The structure was made of A22H steel.

A solid 3D finite element model was used to find the through-thickness stress distribution at the critical weld-toe region to provide a reference against which the effectiveness of the GY2 model could be judged. The linearization of the actual 3D finite element stress field was obtained through numerical processing of the solid 3D finite element data. The maximum and minimum normal stresses determined from the 3D finite element model were $\sigma_{max} = 16.87\ psi$ (1 psi = 1/145 MPa) and $\sigma_{min} = -3.25\ psi$ respectively, and the maximum and minimum linearized

stresses were determined to be $\sigma_{hs}^{1} = 9.22\ psi$ and $\sigma_{hs}^{2} = -4.04\ psi$. The axial stress was found to be $\sigma_{hs}^{m} = 2.59\ psi$ and the bending stress was found to be $\sigma_{hs}^{b} = 6.63\ psi$.

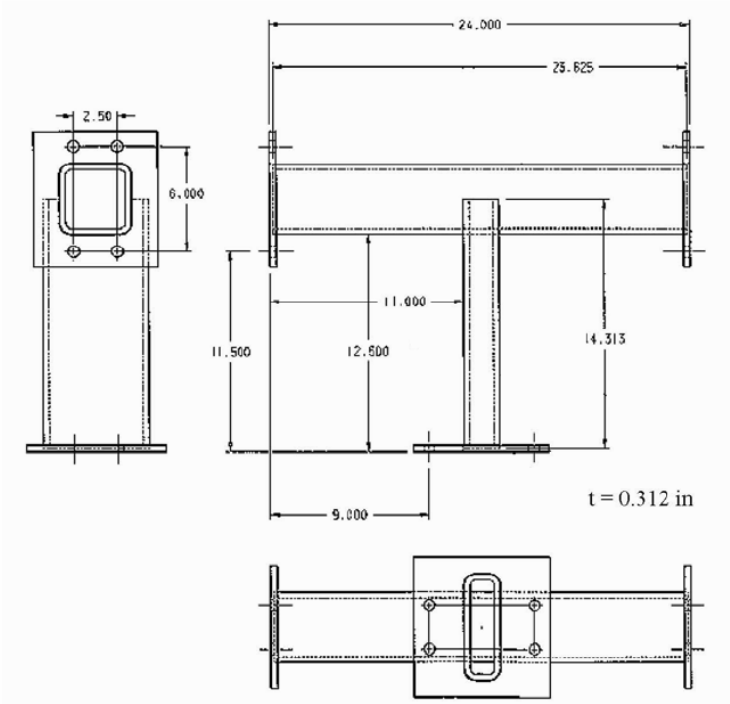

Fig.4 Desmoines welded T-joint and applied load (1 in = 2.54 cm)

The hot spot stresses obtained from the shell model were $\sigma_{hs}^{1} = 8.25\ psi$ and $\sigma_{hs}^{2} = -3.05\ psi$. The hot spot shell membrane and bending stresses were subsequently determined as $\sigma_{hs}^{m} = 2.60\ psi$ and $\sigma_{hs}^{b} = 5.65\ psi$ via equations (5) and (6). In order to determine the peak stress at the weld toe the appropriate stress concentration factors were found. Based on the dimensions of the weld and equations (2) and (3), stress concentration factors $K_{t,hs}^{m} = 1.78$ and $K_{t,hs}^{b} = 2.20$ were obtained. The peak stress $\sigma_{peak} = 17.09\ psi$ was determined using equation (1). As stated previously, the peak stress obtained from the fine mesh 3D finite element model was $\sigma_{peak} = 16.87\ psi$. This value is within 1.3% of the value returned by the finely-meshed 3D solid model.

The stress concentration factors $K_{t,hs}^{m}$ and $K_{t,hs}^{b}$, together with the hot spot shell finite element stresses σ_{hs}^{m} and σ_{hs}^{b}, were subsequently substituted into Monahan's [8] equation (4). The non-linear through-thickness stress distribution in the critical cross section of the weld was determined and plotted against the 3D finite element data (Fig. 5). It was found that both the simulated peak stress and through-thickness stress distribution agreed well with the fine mesh finite element stress data.

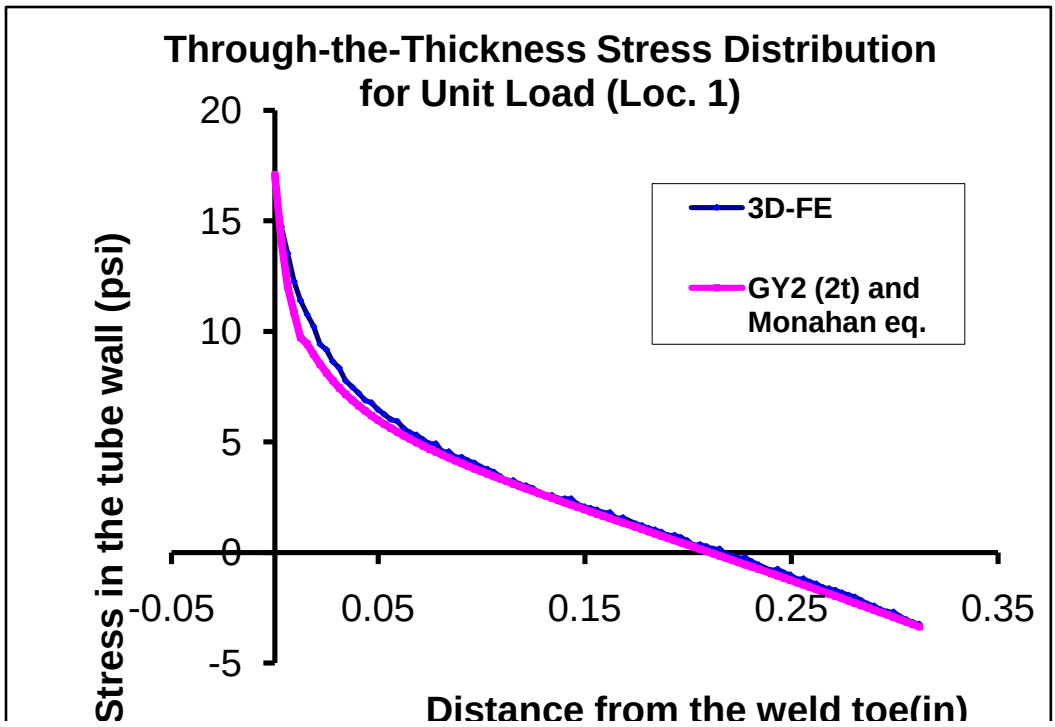

Fig.5 Comparison of the 3D solid finite element stress distribution and the stress distribution obtained using the GY2 method combined with Monahan's equation.

6 Summary

A simple shell finite element model technique for obtaining relevant stress data was presented in the paper. According to the proposed method, an entire structure can be modeled using small number of large shell finite elements.

A procedure for the determination of the magnitude of the peak stress at the weld toe using classical stress concentration factors (one for axial load and one for bending) is described. The approach is based on the decomposition of the hot spot stress into the membrane and bending contributions, and it can be successfully applied to any combination of loading and weld geometry.

The validation of the proposed technique confirmed the accuracy of the proposed method. In the case of the Desmoines T-joint subjected to axial loading (Fig. 4) the shell finite element model overestimated the peak stress by 1.3%. The simulated through-thickness stress distribution based on the hot spot shell finite element model was also in a good agreement with the actual stress distribution obtained from the 3D solid finite element model.

References:

[1] **Marshall, P. W.,** Design of Welded Tubular Connections, *Elsevier*, Amsterdam, 1992

[2] **Dong, P.,** A Structural Stress Definition and Numerical Implementation for Fatigue Analysis of Welded Joints, *International Journal of Fatigue*, 2001, 23, 865-876

[3] **Niemi, E.,** Stress Determination for Fatigue Analysis of Welded Components, *The International Institute of Welding*, Abington Publishing, Cambridge, UK, Doc. IIS/IIW-1221-93, 1995

[4] **V. A. Ryachin and G. N. Moshkariev,** Durability and Stability of Welded Structures in Construction and Earth Moving Machinery (and Road Building Machines), Mashinostroyenie, Moskva, 1984 (in Russian)

[5] **V. I. Trufyakov (editor),** The Strength of Welded Joints under Cyclic Loading, *Naukova Dumka, Kiev,* ed. V. I., 1990 (in Russian)

[6] **J.Y. Young and F.V. Lawrence**, Analytical and Graphical Aids for the Fatigue Design of Weldments, *Fracture and Fatigue of Engineering Materials and Structures*, vol. 8, No.3, 1985, pp. 223-241

[7] **K. Iida and T. Uemura**, Stress Concentration Factor Formulas Widely Used in Japan, *The International Welding Institute*, Document IIW XIII-1530-94, 1994

[8] **Monahan, C. C.,** *Early Fatigue Cracks Growth at Welds*, Computational Mechanics Publications, Southampton UK, 1995

[9] **Fayard, J. L., Bignonnet, A. and Dang Van, K.,** Fatigue design criteria for welded structures, *Fatigue and Fractures of Engineering Materials and Structures*, 1996, 19, iss.6, 723-29